Fusion Engineering and Design 217 (2025) 115122

Contents lists available at ScienceDirect

Fusion Engineering and Design

journal homepage: www.elsevier.com/locate/fusengdes

Electromagnetic design optimization of the inboard shielding blanket for the volumetric neutron source

Ivan Alessio Maione [a,*], Christian Bachmann [b], Irene Pagani [c], Riccardo Lombroni [d]

[a] *Karlsruhe Institute of Technology (KIT), Hermann-von-Helmholtz-Platz 1, 76344 Eggenstein-Leopoldshafen, Germany*
[b] *EUROfusion PMU, Boltzmannstraße 2, 85748 Garching, Germany*
[c] *LT Calcoli srl, Via Bergamo 60, 23807 Merate (LC), Italy*
[d] *University of Tuscia, Largo dell'Università, Viterbo, 01100, Italy*

ARTICLE INFO

Keywords:
Volumetric neutron source
Blanket
Plasma disruptions
EM loads

ABSTRACT

This work presents a set of electromagnetic (EM) analyses performed on the Volumetric Neutron Source (VNS), a facility designed to test fusion reactor components under near-reactor conditions. The study investigates eddy currents, Lorentz forces, and halo current distributions in critical components such as the shield blanket, divertor, vacuum vessel, and thermal shield under transient electromagnetic scenarios. Key events such as Vertical Displacement Events (VDEs), analyzed using MAXFEA, and toroidal field coil fast discharges (TFCFDs) are implemented in finite element method models developed in ANSYS to calculate the induced EM loads.

Focus is given to the inboard blanket's design, with modifications to reduce EM loads by optimizing electrical contacts, refining material configurations, and incorporating ferromagnetic elements to satisfy the requirements for the attachment system. Results provide essential feedback for structural improvements and advancing the VNS toward operational feasibility. The methodology and findings contribute broadly to fusion reactor design by addressing critical challenges posed by EM transients.

1. Introduction

The pursuit of sustainable fusion power hinges on advancing Breeding Blanket (BB) technology, a critical component of fusion reactors responsible for tritium breeding and heat extraction [1]. Currently at a low maturity level, with no operational BBs tested to date, this technology faces feasibility concerns across all considered concepts [2]. Substantial research and development efforts are deemed necessary to overcome these challenges. A proposed solution involves introducing a Volumetric Neutron Source (VNS) [3] for parallel testing and qualification of breeding blankets alongside ITER[4] and DONES[5]. The VNS will offer an experimental environment capable of replicating the neutron flux and fluence conditions expected in full-scale fusion reactors. By enabling extensive component validation, the VNS serves as an essential bridge between experimental research and industrial-scale applications.

The VNS is based on the tokamak configuration. As such, it shares the challenges posed by electromagnetic (EM) transients such as plasma disruptions. Events like Vertical Displacement Events (VDEs) followed by a plasma disruption generate significant induced currents in the conductive structures of the VNS and respective electromagnetic forces due to their interaction with the high magnetic field. These forces must be carefully evaluated to ensure the structural integrity of the in-vessel components. Past studies on tokamaks, including ITER and DEMO, highlight the critical role of EM analysis in addressing these challenges [6–10].

This paper is based on the work done within the EUROfusion consortium on the electromagnetic modeling and optimization of the VNS. Magnetic field distribution, eddy currents and respective Lorentz forces are evaluated considering demanding transients like toroidal field coil fast discharges (TFCFD) and VDEs. The possible presence of ferromagnetic materials, such as EUROFER97[11], is also taken into account. The results of these analyses provide feedback for structural improvements and component optimization. In particular, in this paper, the optimization of the shield blankets in order to comply with the requirements of their attachments on the vacuum vessel (VV) is presented.

2. EM model

The electromagnetic modeling of the VNS follows the well

* Correspondence author.
E-mail address: ivan.maione@kit.edu (I.A. Maione).

https://doi.org/10.1016/j.fusengdes.2025.115122
Received 8 January 2025; Received in revised form 20 March 2025; Accepted 23 April 2025
Available online 5 May 2025

established methodology applied for calculating EM loads in tokamaks as already reported in different papers [8,12,13]. Therefore, this methodology is only briefly summarized here.

The EM model, as depicted in Fig. 1, has been developed in ANSYS and represents a 30-degree toroidal sector of the VNS. This sector is the minimum angular segment required to maintain the cyclic symmetry of the components while effectively reducing computational overhead. The finite element model includes an extensive air region surrounding all conductive structures, extending radially up to 40 m from the machine's axis. This boundary ensures that a flux-parallel condition can be reliably applied at the model's boundaries.

The model incorporates all major structural and functional components, including the upper, equatorial, and lower ports, the five shield blanket modules (two inboard and three outboard), the vacuum vessel, the divertor system, and the vessel's thermal shield.

Additionally, the model accounts for all significant sources of magnetic fields: the plasma, central solenoid (CS), poloidal field (PF) coils, and toroidal field (TF) coils.

The plasma representation in the model is designed to accurately reproduce its electromagnetic effects while maintaining computational efficiency. The primary inputs for representing the plasma include its toroidal current, the toroidal magnetic flux, and the halo currents. Since the focus is on calculating electromagnetic loads on conductive structures rather than analyzing the magnetic field distribution within the plasma, an optimized strategy has been developed, as detailed in the previously referenced papers. With reference to Fig. 1, this approach consists of three key elements:

- An equivalent set of current filaments (PFV). These filaments generate the same magnetic field as the plasma outside a coupling surface near the FW (for plasma poloidal field generation). The currents applied to the filaments are provided as input at each time step by the plasma disruption group.
- A 'fictitious' toroidal solenoid (TFV). Placed in the center of the plasma region, this solenoid is fed by a current distribution that generates the plasma toroidal flux variation caused during the disruptive event. The current to be applied to the solenoid is calculated in pre-processing through ANSYS macros.
- A 'near-node' approach for interpolating halo currents into 3D structures. A 2D point cloud, along with the magnitude of the halo current at each point, is provided as input for the plasma-related halo current representation. This data is then pre-processed using a custom ANSYS macro and mapped onto the nodes of the FW wetted area based on a minimum-distance criterion.

This approach decouples the volumetric distribution of the plasma current during disruptions within the plasma region, enabling accurate reproduction of each disruption's contribution without modifying the mesh.

Together, these elements provide a comprehensive framework for simulating electromagnetic interactions within the VNS.

2.1. Blanket model

Fig. 2 illustrates the structure of an inboard blanket segment as implemented in the EM model. With reference to the CAD section depicted in Fig. 2(a), the segment features a welded box structure composed of the back supporting structure, side walls, and first wall, reinforced internally by stiffening ribs. These ribs define six distinct regions for the placement of shielding material. As shown on the right side of Fig. 2(c), these shielding regions are poloidally divided into four sections. In each shielding region, shielding blocks of W or EUROFER have been placed which are connected to the toroidal-radial ribs via structural pillars. For convenience, and given their similarity in position and material properties, the shielding blocks have been grouped into eight ANSYS components (IBL_SB1 to IBL_SB8), as indicated in Fig. 2(d).

Building on an initial estimation of the structural geometrical dimensions from preliminary structural and thermohydraulic analyses, the shield blanket design has been refined to minimize the Lorentz loads. Key improvements, developed alongside structural evaluations detailed in [14], include electrically isolating the shielding blocks from the supporting structure (modeled by applying a non-conductive material to the IBL_PILLAR components), and reducing thicknesses as follows: the first wall from 40 mm to 35 mm, the side walls from 28 mm to 15 mm, and the back supporting structure from 40 mm to 24 mm. Additionally, non-conductive yet shielding materials have been incorporated into specific sections of the back supporting structure (see Fig. 2(a)), and the

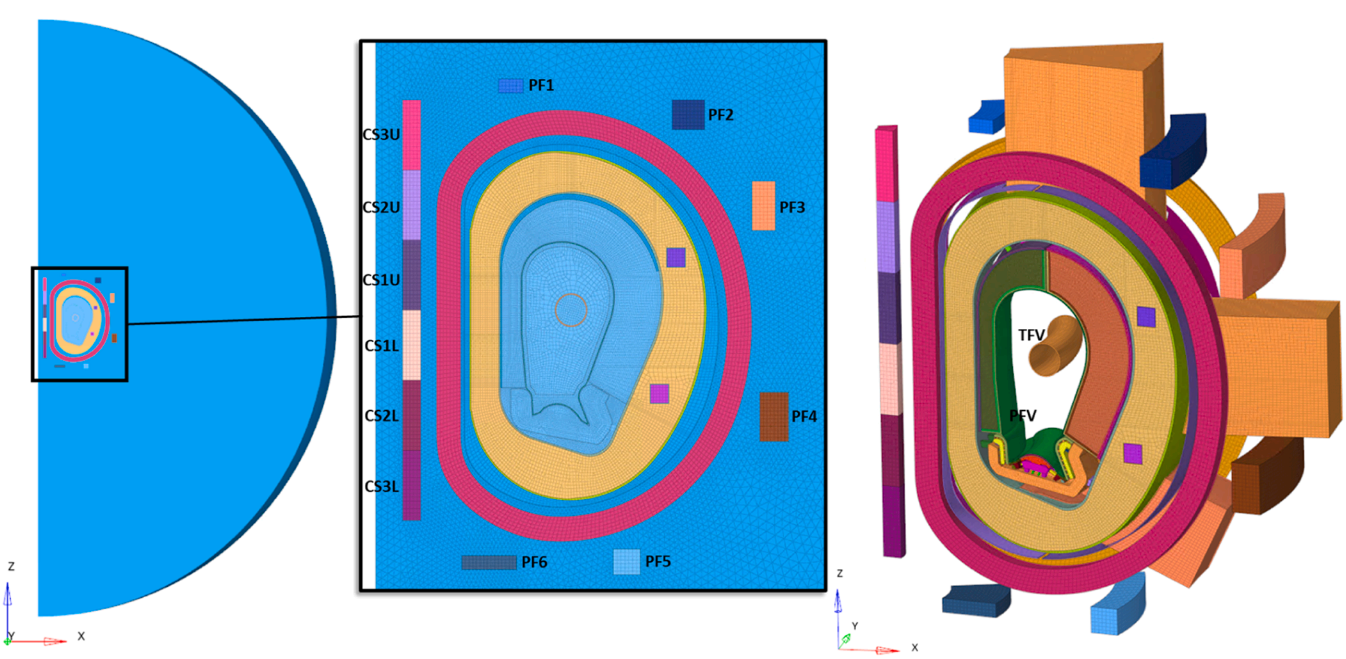

Fig. 1. Detail of the EM model for the VNS: (left) full model with enclosure, (center) close-up view of the magnetic cage, (right) overview of conductive components and magnetic field sources.

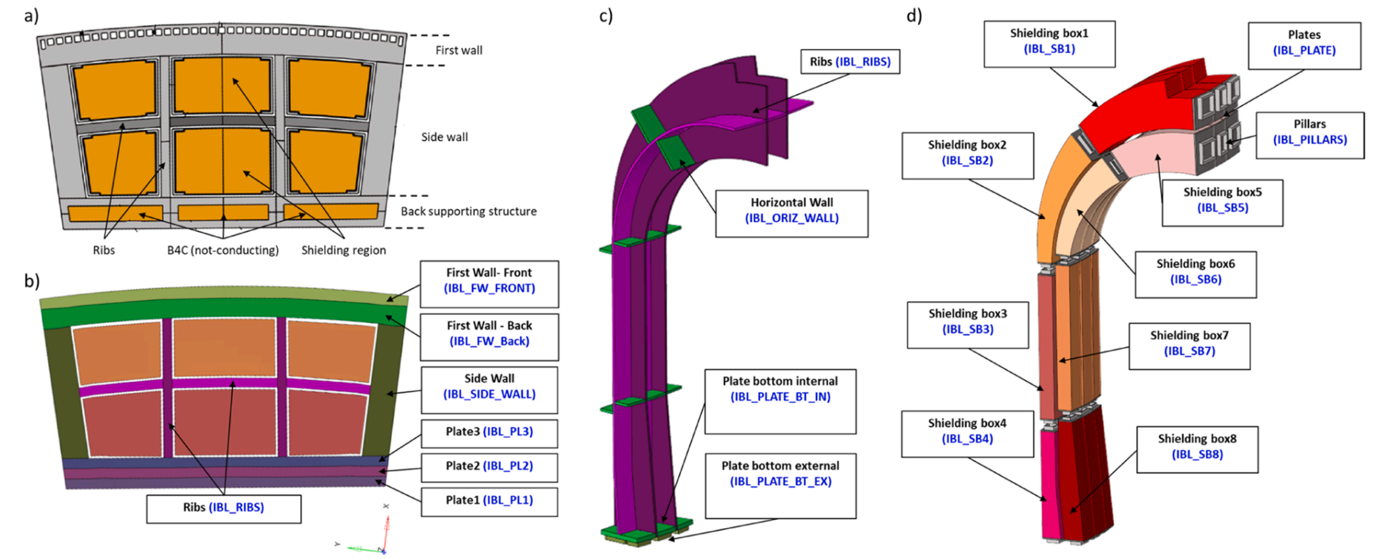

Fig. 2. Detailed view of the internal structure of the inboard shielding blankets as implemented in the EM model. On the right, a comparison of the IBL equatorial cross-section is shown, with the reference CAD model (a) and its corresponding representation in the EM model (b). On the left, a poloidal view of the internal region highlights the ribs and wall (c) designed for the placement of the shielding blocks (d).

placement of electrical contacts with the vacuum vessel has been optimized (see Section 4.1).

These improvements have been incorporated into the EM model by adjusting the materials' properties, eliminating the need to modify the mesh. Table 1 summarizes the impact of these modifications on the homogenized electrical properties of the initial and improved inboard blanket designs.

3. EM tranients

The EM transients considered in this work are a toroidal field coil fast discharge (TFCFD) and a fast and slow upward VDE (VDEUP).

The discharge of the TFC is modeled imposing an exponential decay of the coil current with a characteristic time of 5 s, while the poloidal coil currents remain constant (see Fig. 3).

On the other side, plasma disruptions have been calculated using MAXFEA code [15] applying the following strategy:

- a small perturbation in radial field is imposed at the beginning of the simulation to excite vertical instability;
- the plasma current is kept constant during the vertical evolution;
- the thermal quench (TQ) is imposed when q95 = 2 a linear plasma poloidal beta drop in 0.2 ms;
- a current spike of 5 % of initial value is imposed during the TQ;
- current quench (CQ) follows lasting 4.2 ms and 47.3 ms for the VDEUP fast and slow, respectively.

Integral parameters for the two considered VDEUPs are reported in Fig. 4.

Table 1
Equivalent Inboard Shield Blanket materials' electrical properties (initial and improved configuration). Differences between the two configuartions are reported in red.

Component name	Material	Temp (°C)	ρx (μΩ m) initial	ρx (μΩ m) improved
IBL_CHIM	SS316	100	0.799	0.799
IBL_CONN_LW	SS316	50	0.765	0.765
IBL_CONN_UP	SS316	50	0.765	0.765
IBL_FW_FRONT	SS316	85	1.217	1.217
IBL_FW_BACK	SS316	85	0.789	0.968
IBL_ORIZ_WALL	SS316	60	0.772	0.772
IBL_PILLARS	SS316	60	1.328	–
IBL_PIPES	SS316	50	1.078	1.078
IBL_PL1	SS316	90	1.075	1.390
IBL_PL2	SS316	90	0.053	1.390
IBL_PL3	SS316	90	1.052	1.390
IBL_PLATE	SS316	60	0.772	0.772
IBL_PLATE_BT_EXT	SS316	60	0.785	0.785
IBL_PLATE_BT_IN	SS316	60	0.527	0.527
IBL_RIBS	SS316	60	0.772	0.772
IBL_SB1	EUROFER97	80	0.574	0.574
IBL_SB2	EUROFER97	80	0.574	0.574
IBL_SB3	W	75	0.065	0.065
IBL_SB4	EUROFER97	80	0.574	0.574
IBL_SB5	W	75	0.065	0.065
IBL_SB6	W	75	0.065	0.065
IBL_SB7	W	75	0.065	0.065
IBL_SB8	W	75	0.065	0.065
IBL_SIDE_WALL	SS316	100	0.999	1.864

4. EM results

In this section, the main electromagnetic results are summarized. Forces and moments acting on each component are calculated relative to a local Cartesian reference frame. This reference frame is centered at the geometric center of the respective component. The z-axis aligns vertically, pointing upward, while the x-axis is aligned radially, pointing outward from the global origin toward the geometric center of the

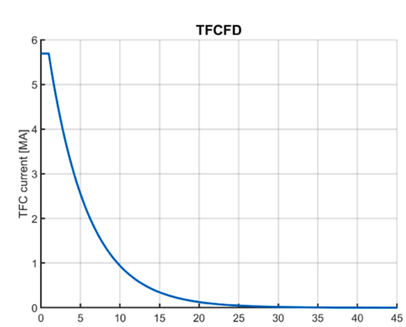

Coil	Current (MA)
CS3U	6.61
CS2U	6.61
CS1U	-1.84
CS1L	-7.34
CS2L	-6.45
CS3L	-2.70
PF1	1.29
PF2	-5.86
PF3	5.84
PF4	7.23
PF5	6.26
PF6	3.72

Fig. 3. Currents in the magnets during the TFCFD.

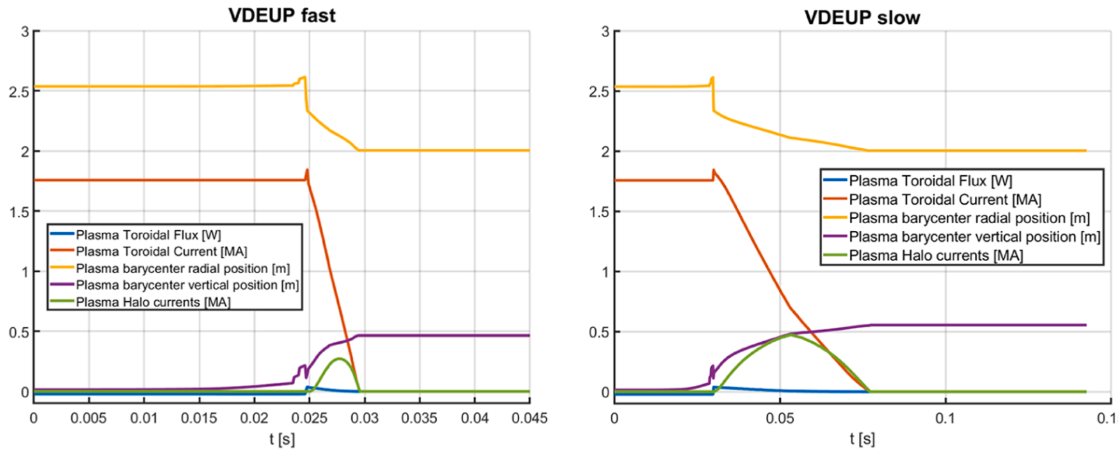

Fig. 4. Integral parameters for the slow and fast VDEUP.

component.

These local frames facilitate consistent comparisons of electromagnetic loads across different components, providing a coherent basis for analyzing load distributions. Such clarity is essential for understanding the implications of these loads on structural design and for informing targeted optimizations.

4.1. Improvement of the electrical contacts configuration

Starting from a DEMO-like configuration for the electrical contacts [10], the position of the upper contacts between the IB segments and the VV was adjusted to reduce the asymmetry in the radial forces experienced by the IBL and IBR. As noted in [16], the DEMO-like configuration, given the symmetry of the IB segments and the compensating forces between the left and right segments, plausibly induces an 'unbalanced' poloidal-toroidal current loop in the structure.

With the new configuration, which places the electrical contacts symmetrically at the top of the inboard blankets, a significant reduction in poloidal forces (both radial and vertical) on each segment is achieved, as shown in Fig. 5.

4.2. Ferromagnetic loads

The inclusion of ferromagnetic material, specifically EUROFER97, is an intentional design choice that has been applied only to the inboard blankets. The interaction of this material with the high toroidal magnetic field induces a radial force that effectively pushes the inboard blankets toward the vacuum vessel (VV) inner shell, providing the necessary mechanical support between the blanket and the VV. This design strategy aligns with the approach previously investigated in the DEMO project, as detailed in [10].

During the analyzed plasma disruptions, the ferromagnetic loads remain relatively constant. The radial force, predominantly negative, is approximately 450 kN. In addition to the radial force, a negative toroidal moment of approximately 90 kN occurs due to the intentional uneven distribution of ferromagnetic material, as reported in Fig. 6.

4.3. Comparison of lorentz loads for various design options

As detailed in Section 2.1, the blanket design has been optimized to mitigate the EM loads that were identified as critical for the attachment system. During plasma disruptions, these loads tend to exert forces that "open" the attachment supports, as demonstrated in [14]. To illustrate the impact of these design improvements, Fig. 7 provides a comparison of the total force and moment acting on the IBL segment during a fast VDEUP for both the initial and improved configurations. Additionally, to highlight the role of the shielding blocks (SBs), which are composed of tungsten and therefore exhibit low resistivity, the comparison has been extended to include a configuration without SBs.

For the improved configuration, Fig. 8 summarizes the total force and moment peaks, including both maximum and minimum values, acting on the IBL during the three analyzed EM transients. The force graph reveals that while the peak magnitudes vary across the transients, the forces remain predominantly radial, highlighting the significant influence of the ferromagnetic component. Notably, the radial force experiences substantial fluctuations during the TFCFD scenario, primarily due to the interplay between the generation of poloidal eddy currents and the decrease in the toroidal magnetic field, the latter being

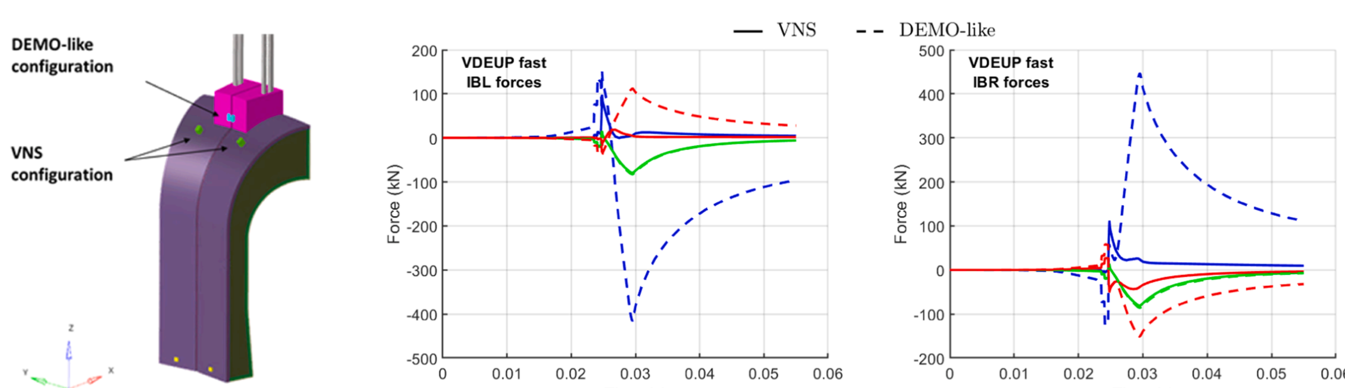

Fig. 5. Comparison of the total force on the IBL and IBR due to eddy current-induced Lorentz forces during a fast VDEUP, considering two electrical contact configurations: (i) DEMO-like design and (ii) VNS design.

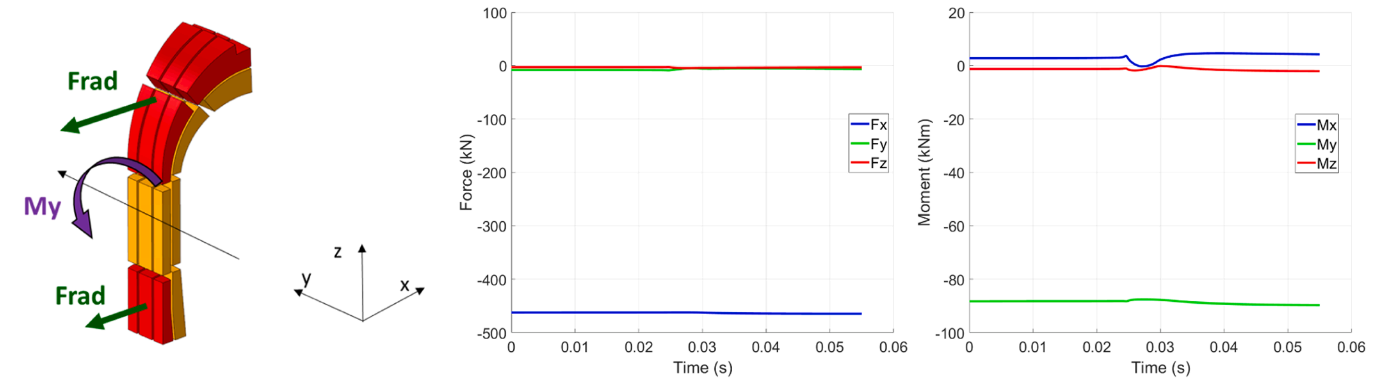

Fig. 6. Ferromagnetic loads (force and moment relative to the local coordinate system) acting on the IBL segment during a VDEUP fast event.

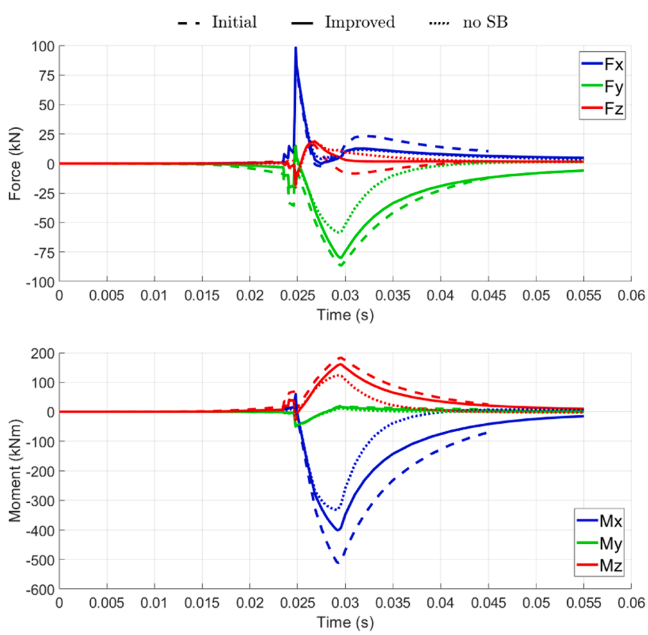

Fig. 7. Comparison of the total force and moment acting on the IBL segment due to eddy currents induced during a fast VDEUP for the initial design, the improved design, and a hypothetical design without shield blocks (no SB).

	Fx-max [kN]	Fx-min [kN]	Fy-max [kN]	Fy-min [kN]	Fz-max [kN]	Fz-min [kN]
VDEUP fast	-363.95	-462.46	6.11	-85.46	14.39	-21.21
VDEUP slow	-363.91	-465.37	6.11	-37.07	-0.67	-21.31
TFCFD	-10.49	-678.22	2.65	-8.9	34.57	-1.78

	Mx-max [kNm]	Mx-min [kNm]	My-max [kNm]	My-min [kNm]	Mz-max [kNm]	Mz-min [kNm]
VDEUP fast	62.8	-399.55	-71.76	-138.59	160.01	-29.34
VDEUP slow	62.69	-130.63	-72.84	-138.5	59.06	-29.35
TFCFD	3.8	-0.6	-10.6	-90.17	-0.61	-7.43

Fig. 8. EM load peaks (max and min) acting on the IBL during the considered EM transients.

the main author for the ferromagnetic radial force.

The most significant moments are generated about the radial and vertical axes by the interaction between the eddy current loops flowing in the radial-toroidal cross-section of the blanket crossing the toroidal magnetic field. These current loops are primarily driven by variations in the toroidal plasma current (and are therefore absent during the TFCFD), with their intensity being highest during the fast VDEUP.

4.4. Halo current contribution

Poloidal halo currents enter/exit the in-vessel components on the plasma-facing surfaces wetted by the halo region of the disrupting plasma. The wetted areas change during the course of the disruption transient. The central-upper part of the inboard blankets is expected to be wetted during an upward VDE, see Fig. 9.

As shown in Fig. 10, the electromagnetic loads resulting from halo currents primarily consist of (i) radial-vertical forces, caused by the interaction of the poloidal current with the toroidal magnetic field, and (ii) a toroidal moment arising from the force distribution relative to the blanket's geometrical center. In general, halo current-induced EM loads are higher during the slow event compared to the fast event, primarily because the halo current magnitude is greater in the slow case. Additionally, these loads are lower in magnitude than those generated by eddy currents induced in the blanket due to the fast decay of the large plasma current during disruptions.

5. Conclusions

The results of the electromagnetic analyses have provided essential support for the preliminary assessment of the VNS components, delivering detailed EM load evaluations for various demanding transient scenarios. Furthermore, the study has played a key role in refining the shield blanket design through effective synergy with structural analysis.

The optimization of the electrical contacts between the blankets and

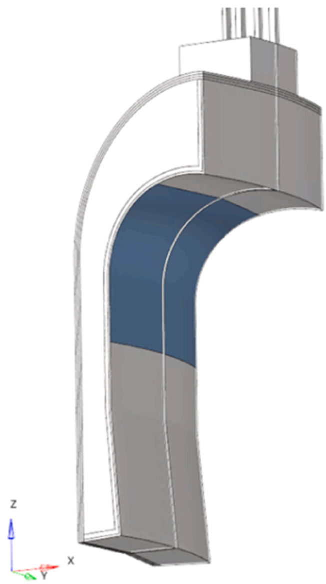

Fig. 9. Inboard blankets plasma wetted region (in blue) during a slow VDEUP.

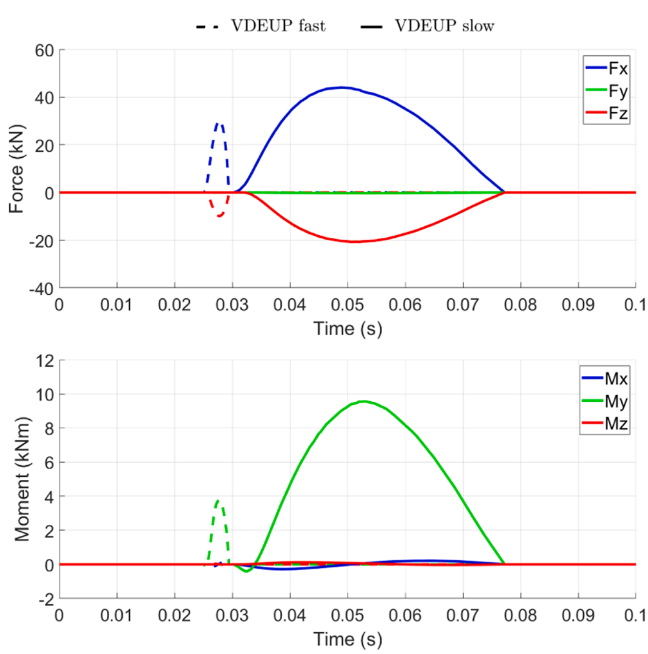

Fig. 10. Electromagnetic forces and moments on the IBL due to Halo currents during a VDEUP: fast vs. slow event.

the vacuum vessel has significantly reduced the radial forces caused by poloidal eddy currents on the inboard blankets during VDEs. However, this optimization did not impact the radial/vertical moments, which are associated with toroidal-radial eddy current loops and remain critical for the attachment system. To mitigate this issue, specific IB design changes have been implemented leading to a ~20 % decrease in the peak moments. However, as reported in [14], this reduction is still insufficient to ensure proper mechanical support of the blanket during a fast VDE. The significance of halo currents was found to be relatively low in the analysed scenarios.

Future work will aim at simulating additional EM transients, such as VDE down events, and at further optimizations of the blanket structure and ferromagnetic inserts to fully meet the requirements of the attachment system.

CRediT authorship contribution statement

Ivan Alessio Maione: Writing – original draft, Supervision, Methodology, Investigation, Conceptualization. **Christian Bachmann:** Writing – review & editing, Supervision, Project administration, Funding acquisition. **Irene Pagani:** Writing – review & editing, Visualization, Software, Resources, Methodology, Investigation, Formal analysis, Data curation. **Riccardo Lombroni:** Writing – review & editing, Methodology, Formal analysis, Data curation.

Declaration of competing interest

The authors declare the following financial interests/personal relationships which may be considered as potential competing interests: Ivan Alessio Maione reports financial support was provided by European Consortium for the Development of Fusion Energy. If there are other authors, they declare that they have no known competing financial interests or personal relationships that could have appeared to influence the work reported in this paper.

Acknowledgments

This work has been carried out within the framework of the EUROfusion Consortium, funded by the European Union via the Euratom Research and Training Programme (Grant Agreement No 101052200 — EUROfusion). Views and opinions expressed are however those of the author(s) only and do not necessarily reflect those of the European Union or the European Commission. Neither the European Union nor the European Commission can be held responsible for them.

Data availability

The data that has been used is confidential.

References

[1] G. Federici, et al., An overview of the EU breeding blanket design strategy as an integral part of the DEMO design effort, Fusion Eng. Des. 141 (2019) 30–42.
[2] Francisco A. Hernández, et al., Advancements in designing the DEMO driver blanket system at the EU DEMO pre-conceptual design phase: overview, challenges and opportunities, J. Nucl. Eng. 4 (3) (2023) 565–601, https://doi.org/10.3390/jne4030037, 2673-4362.
[3] C. Bachmann, et al., in: , Dublin, Ireland, 2024, pp. 22–27. Sept.
[4] https://www.iter.org/ (accessed May 1, 2025).
[5] https://ifmif-dones.es/ (accessed May 1, 2025).
[6] S. Pak, et al., Electromagnetic load calculation of the ITER machine using a single finite element model including narrow slits of the in-vessel components, Fusion Eng. Des. 88 (2013) 3224–3237.
[7] P. Testoni, et al., F4E studies for the electromagnetic analysis of ITER components, Fusion Eng. Des. 89 (2014) 1854–1858.
[8] I.A. Maione, et al., Electromagnetic analysis activities in support of the Breeding Blanket during the DEMO Pre-conceptual Design phase: methodology and main results, Fusion Eng. Des. 166 (2021) 112285.
[9] M. Richiusa;, et al., The integrated engineering design concept of the upper limiter within the EU-DEMO LIMITER system, Fusion Eng. Des. (2024) 202.
[10] C. Bachmann, et al., Mechanical support concept of the DEMO breeding blanket, Fusion Eng. Des. 173 (2021) 112840.
[11] K. Mergia, et al., Structural, thermal, electrical and magnetic properties of Eurofer 97 steel, J. Nucl. Mater. 373 (2008) 1–3.
[12] I.A. Maione, et al., Analysis of EM loads on DEMO WCLL breeding blanket during VDE-up, Fusion Eng. Des. 136 (2018) 1523–1528.
[13] I.A. Maione, et al., Investigation of electromagnetic sub-modeling procedure for the breeding blanket system, J. Nucl. Eng. 4 (2023) 165–176.
[14] F. Viganò, et al., Thermo-Structural FE analysis design and optimization of Volumetric Neutron Source Tokamak components, 33rd Symposium on Fusion Technology, Dublin, Ireland, 2024, pp. 22–27. Sept.
[15] R. Lombroni, et al., Using MAXFEA code in combination with ANSYS APDL for the simulation of plasma disruption events on EU DEMO, Fusion Eng. Des. 170 (2021) 112697.
[16] I.A. Maione, et al., Update of electromagnetic loads on HCPB breeding blanked for DEMO 2017 configuration, Fusion Eng. Des. 156 (2020).